

Methods for experimental determination of solid-solid interfacial thermal resistance with application to composite materials

Karol Pietrak*, Tomasz S. Wiśniewski

*Institute of Heat Engineering, Warsaw University of Technology
21/25 Nowowiejska Street, 00-665 Warsaw, Poland*

Abstract

Interfacial thermal resistance (ITR) exists between filler and matrix in any composite material and has a significant influence on its effective thermal conductivity. To predict the effective thermal conductivity of composite material, the conductivities of each component as well as the ITR must be known. Theoretical models, like the acoustic mismatch model (AMM), allow for accurate ITR determination only for an idealized case of perfect contact (no interfacial gaps and good bonding). The interfacial bonding in typical composites for thermal conduction, like diamond-reinforced metal matrix composites (MMCs) is usually highly imperfect and the ITR, in composites of the same type, depends highly on the individual manufacturing conditions. Therefore, a great need exists for reliable experimental ITR measurement techniques. In this paper, the main difficulties regarding experimental ITR measurements are discussed. A review of measurement techniques is presented, with the main focus put on the principle of each technique and its appropriateness for the purpose of composite materials. The strengths and weaknesses of each technique are discussed.

Keywords: Interfacial thermal resistance, Thermal boundary resistance, Composite materials, Experimental research

1. Introduction

When heat flows through an interface between the constituents of a composite, a temperature drop ΔT occurs at this interface. This disturbance of heat flow can be described by means of thermal resistance. It is known as interfacial thermal resistance (ITR). The interfacial thermal resistance in a composite refers to the combined effect of two resistances: (a) thermal contact resistance (TCR) due to poor mechanical and chemical bonding between constituent phases

and (b) thermal boundary resistance (TBR) due to differences in the physical properties of the composite's constituents, also known as the Kapitza resistance [1]. There are theoretical models allowing for the prediction of thermal boundary resistance alone, but the thermal contact resistance part is always hard to evaluate. For that reason, accurate methods of experimental ITR evaluation are needed.

In a majority of cases, ITR has a significant influence on the effective thermal conductivity of composite material. Combining two highly conductive materials into a composite, one may obtain a material with thermal conductivity lower than the conductivities of the constituents. That is due to the ITR between the constituents. The negative effect increases when the

*Corresponding author

Email addresses: karol.pietrak@itc.pw.edu.pl
(Karol Pietrak*), tomasz.wisniewski@itc.pw.edu.pl
(Tomasz S. Wiśniewski)

area of the interface per unit volume increases. In order to enhance the effective thermal conductivity of newly designed composite materials it is essential to understand the mechanisms of interfacial heat transfer. This topic will be described further in the next section. Due to the subtle nature of the phenomenon, many difficulties are encountered during ITR measurement attempts. Nevertheless, some experimental techniques have been proposed by several authors. The difficulties regarding ITR measurement are addressed in section 3. In section 4, ITR measurement techniques are presented together with a critical evaluation of them.

2. On the nature of interfacial heat transfer

The interfacial thermal resistance R_{int} may be defined as the ratio of the temperature discontinuity at the interface ΔT to the heat rate \dot{Q} per unit area A flowing across that interface [2]:

$$R_{int} = \frac{\Delta T}{\dot{Q}/A} \quad (1)$$

Now let us consider the causes of the temperature drop at the interface. First of all there is the thermal boundary resistance due to the difference in the properties of contacting mediums. Heat in a solid may be carried as a vibration of an atomic lattice (phonon transport) or by free electrons (electronic transport). Different mediums (materials) possess different vibrational and electronic properties. A heat carrier (electron or phonon), arriving at the interface, reaches a physical end of the medium in which it originally propagates and must fulfill certain requirements to continue its propagation in the other medium. Not all heat carriers will pass, even if the mechanical contact between the two phases is perfect.

Let us consider phonon transport alone. The value of TBR depends on the probability of the transmission, the number of phonons incident on the interface and the energy carried by each phonon. The hard part is to calculate the probability. Two basic models have been proposed to calculate this probability—the acoustic mismatch model (AMM) and the diffuse mismatch model (DMM).

In the acoustic mismatch model the interface is assumed to be planar and the materials in which phonons propagate are treated as continua (no lattice). The latter assumption is accurate for phonons with wavelength much greater than typical interatomic spacings. A phonon arriving at the interface may specularly reflect, reflect with mode conversion, refract, or refract with mode conversion. The transmission probability is the total fraction of the energy transmitted across the interface and it is determined on the basis of the laws of continuum acoustics (for more details, see [2]).

The AMM model assumption is that there is no scattering of phonons at the interface. However, various experiments show that scattering occurs at real interfaces and it influences the value of TBR. The diffuse mismatch model was proposed by Swartz and Pohl [2] in response to these observations. In the DMM the assumption of complete specularity is replaced with the opposite extreme: all the phonons are diffusely scattered at the interface. This leads to an upper limit of the effect that diffuse scattering can have on boundary resistance. In the diffuse mismatch model, acoustic correlations at interfaces are assumed to be completely destroyed by diffuse scattering, so that the only determinants of the transmission probability are densities of phonon states and the principle of detailed balance. The statement of the principle of detailed balance for interfacial heat transfer is as follows: in thermal equilibrium, the number of phonons of a given phonon state (polarization and wave vector) leaving one side is the same as the number of phonons returning from the other side into that state [2].

The above mentioned models are quite important historically, yet their predictions of solid-solid TBR are accurate only for cryogenic temperatures (best below a few K). For 50 K the discrepancy between measured and predicted TBR is one order of magnitude and it increases with temperature. Further development resulted in the formulation of the more accurate scattering mediated acoustic mismatch model (SMAMM) by Prasher and Phelan [3]. It reduces to AMM for low temperatures and allows for better prediction of TBR at high temperatures thanks to the scattering-time-dependent fitting parameter. However, the fitting parameter, requires experimental de-

termination.

It should be emphasized that, in these models, only phonon transport is considered and they apply to cases in which at least one of the contacting solids is dielectric. The AMM and DMM assume the near-interfacial region to be quite ideal and defectless, and hence they apply to cases in which thermal boundary resistance plays a dominant role in the overall ITR (the contact resistance part is negligible). In the case of technical composite materials, numerous types of imperfections may occur at the interface, which increase the scattering of heat carriers. These include localized atomic disorder, lattice distortions, regions in which interdiffusion of contacting solids occurred, and layers of corroded material and interfacial gaps [4]. It is obvious that these phenomena result in greater ITR. Only in the SMAMM is simplified inclusion of the effects of such additional near-interface scattering possible via the fitting parameter.

Molecular-dynamics (MD) simulation can be used to compute ITR numerically. First of all, we must build an atomistic model of the interface of interest. This type of modeling involves integration in time of Newton's equations of motion for an ensemble of atoms interacting with each other through a, usually empirical, interatomic potential. Because the formalism of the MD approach does not require any a priori understanding of heat transport, it is ideal for investigating the fundamental heat-transfer mechanisms themselves. However, MD does have the significant limitation of being entirely classical, with each vibrational mode equally excited; thus it is only rigorously applicable to solids above the Debye temperature. Moreover, since electrons are not included in an atomistic model, it is not possible to simulate electrical conductors or the electron-phonon interactions present in many semiconductors [5].

3. The subtleties of ITR measurement

Firstly, let us focus on cases where mechanical contact between the two phases is good, meaning that we measure the TBR component alone. To measure the TBR for a given interface, the temperature discontinuity $\Delta T = T_2 - T_1$ has to be determined, where T_1 and T_2 are the temperatures of phonons incident on the respective sides of the interface. The place-

ment of thermometers should assure that temperatures of appropriate distributions of phonons are being recorded—the incident phonons on both sides of the interface. Also, the thermometers must be placed as close to the interface as possible. Otherwise, it may be necessary to subtract the temperature gradient in the material from the measured value to obtain the temperature at the interface. Such correction generates additional uncertainty. The general principle is that the measured temperature is correct if the thermometer distance from the interface is much less than the phonon mean-free path for the given material [2].

For pure metals, there are no significant problems with thermometry, at least at temperatures below a few K. In these materials, because electrons dominate the heat transport and strongly scatter the phonons, the phonon distribution is isotropic. The total phonon distribution and the distribution of phonons incident on the interface have the same temperature. Since electrons dominate the thermal transport, phonon scattering at the thermometer will not affect the temperature measurement. In TBR measurements, the positioning of thermometers usually is critical if one side of the interface is a dielectric. At temperatures below 1 K, in dielectric crystals, the mean free path is often determined by the condition of the surfaces and the size and positions of thermometers on the crystal, yet the thermometers must be placed within a phonon mean-free-path length of the interface. If the thermometers scatter phonons so strongly that they significantly influence the mean free path, there may be no reasonable place to put the thermometers [2].

Phonon mean-free paths, for any material, diminish rapidly with increasing temperature, while the thermal resistance of the bulk increases. Above a few K the placement of thermometers allowing direct measurement of desired phonon temperatures becomes difficult or impossible, and it becomes necessary to subtract bulk thermal gradients from the measured ΔT between the thermometers [2]. In Fig. 1 an appropriate placement of thermometers for temperatures around a few K is presented. Consider the characteristic placement for the dielectric side of the interface. It serves the purpose of measuring the temperature of incident phonons distribution only. For

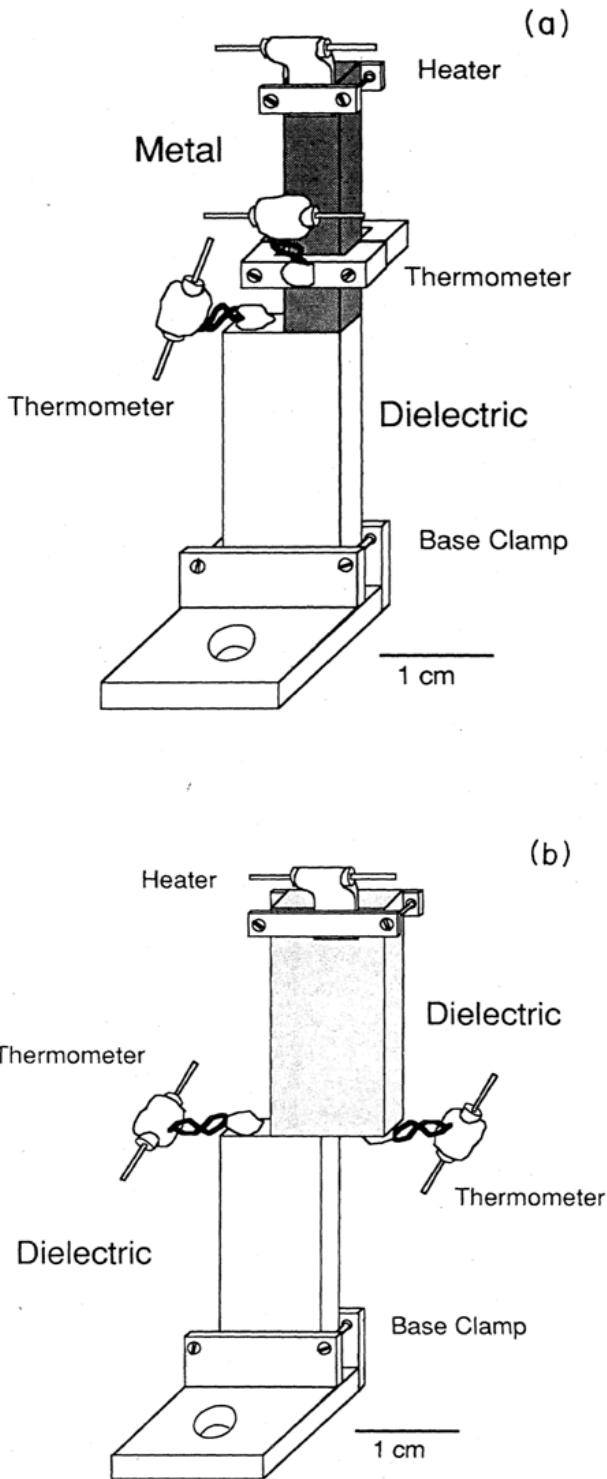


Figure 1: Setup for thermal boundary resistance measurement, between two solid materials, in temperatures around a few K (Reprinted figure with permission from [2]. Copyright © 1989 by the American Physical Society)

the metal side it is not required.

Contact methods of thermometry, utilizing a ther-

mal probe (a thermometer, thermocouple etc.) placed in the interesting point of the sample is generally not sufficient when measuring ITR. That is due to the parasite probe-sample thermal resistance, which is of the order of the measured interfacial thermal resistance. For that reason, scanning thermal microscopy (SThM) cannot be used to measure ITR in composite materials, although it fulfills the need for high spatial resolution [6]. This flaw may be worked around by using contactless methods of temperature measurement. Infrared sensors and optical methods are being utilized successfully. These methods will be discussed in more detail in the next section.

Due to the difficulties concerning direct measurement of interfacial thermal resistance in composite materials, indirect methods are used widely. Most of these are ITR estimations based on the measurement of the effective thermal conductivity [7–12]. The accuracy of such ITR estimation depends on the appropriate choice of model and its adaptation to the specific problem. On the other hand, a wide range of effective thermal conductivity models incorporating ITR are available and new ones are appearing.

4. Experimental methods of ITR measurement

4.1. Swarz and Pohl method

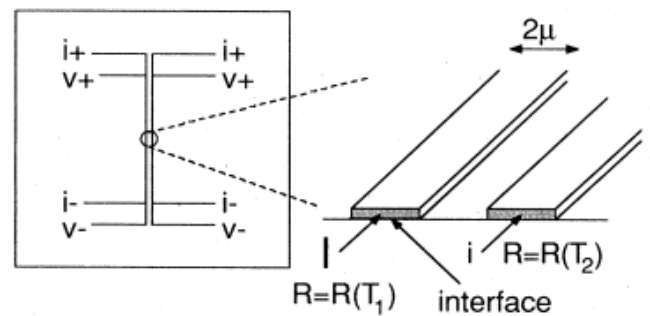


Figure 2: The experimental setup proposed by Swarz and Pohl to measure the ITR between metals and dielectrics (Reprinted figure with permission from [2]. Copyright © 1989 by the American Physical Society). Substrate dimensions: $1 \times 1 \times 0.025 \text{ cm}^3$. Length of the metal strips: 2.5 mm

Miniaturization of the experimental device and sample is one of the possible ways of making it easier to measure temperatures on both sides of the interface. Geometry utilizing the profits of miniaturization was proposed by Swarz and Pohl, who measured

the ITR of various metals on dielectric substrates in temperatures 1...300 K [13]. The experimental device is presented in Fig. 2.

Two thin strips of metal are vapor-deposited onto the surface of dielectric plate (the substrate). The electrical resistance R of both metal strips is temperature-dependent and therefore both can be used as thermometers. One of the strips is heated by a relatively large electric current I . Its temperature is slightly higher than that of the substrate below. The interface of interest is between that strip and the substrate. Through the second strip flows a smaller electric current i . It does not produce significant heat, and therefore the strip temperature is equal to the temperature of the substrate below. The second strip measures the temperature of the substrate.

For temperatures below 50 K it can be assumed that the temperature of the substrate under the heated strip is equal to that measured by the second strip. For higher temperatures, the temperature of the substrate below the Joule-heated strip must be calculated by solving a time independent heat equation (Laplace equation) given the temperature measured by the other strip. This is required because the difference between the two becomes significant. The temperatures of the phonon distributions incident on the two sides of the interface are measured, as required for the measurement to correspond to the definition of ITR. Due to the high conductivity of metal film and its thinness, the temperature distribution within it is uniform. The method has been successfully used by other researchers [14] and enabled the influence of disordered lattice regions on the ITR between metals and dielectrics to be examined.

4.2. Transient thermorefectance

This type of experimental ITR estimation employs the contactless optical method of temperature measurement and is used mainly for metal-dielectric interfaces. The sample takes the form of a thin metallic film deposited onto a dielectric substrate. The film is heated by a short laser impulse (the pump). After partial absorption of the impulse energy there is a small increase in the film temperature. Then, the film cools down as the heat is transferred through the interface to the dielectric substrate. The change in temperature of the metal $\Delta T(t)$ is accompanied by

a small change in its optical reflectivity $\Delta r(t)$. Since the reflectivity of metals varies slowly with temperature, we can assume that $\Delta T(t) \sim \Delta r(t)$. Reflectivity change is measured by the second laser beam (the probe beam) which is delayed relative to the pump beam. This allows the temporal cooling profile of the sample to be recorded. In fact, the intensity of the laser beam reflected off the surface of the metal film is measured by a photodiode detector.

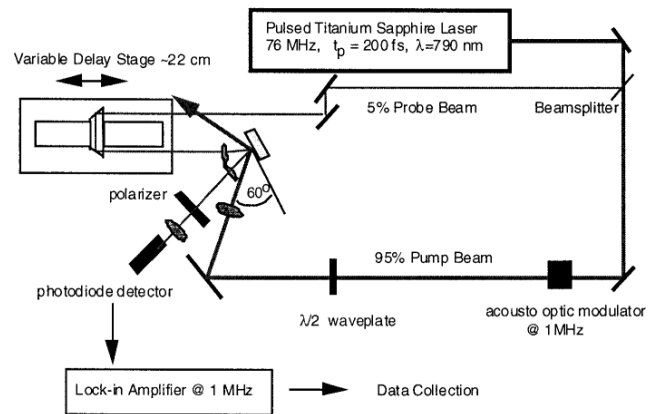


Figure 3: Experimental setup for the transient thermorefectance (TTR) technique (Reprinted by permission of the publisher from [15]. Published by Taylor & Francis Ltd, <http://tandf.co.uk/journals>). Example from [15]

A typical experimental setup is presented in Fig. 3. The technique uses pulses generated by a femtosecond laser. Typical FWHM pulse width is of the order of 200 fs. A nonpolarizing beam splitter separates the laser beam into two beams with an intensity ratio of 20:1. The pump beam passes through an acousto-optic modulator, which creates a pulse train at a frequency of 1 MHz. A half-wave plate rotates the heating beam's polarization parallel to the plane of incidence. The pump beam is focused to a diameter of 10–50 μm at an incident angle of 30°. The s-polarized probe beam passes through a dove-tail prism mounted on a variable delay stage that can be adjusted to obtain the required time delay. The probe beam is focused to $\sim 5 \mu\text{m}$ at near-normal incidence to minimize the illuminated area. Light gathered by the silicon photodiode is filtered by a polarizer set to pass only s-polarized light. The detector's response is filtered by a lock-in amplifier at a frequency of 1 MHz [15].

The obtained TTR signal record represents the

cooling curve of the metal film. An example of the recorded TTR signal is shown in Fig 4. By fitting the theoretical curve, which stems from the thermal model, to the measured curve, one can obtain the value of ITR. The heat transfer in the sample may be described by equations [16]:

$$c_f d \frac{\partial T_f}{\partial t} = -\Lambda_{Bd} [T_f - T_S(0)] \quad (2)$$

$$c_s \frac{\partial T_S(z)}{\partial t} = \lambda_s \frac{\partial^2 T_S(z)}{\partial z^2} \quad (3)$$

where d is metal film thickness, T_f is the film temperature (uniform distribution assumption due to the thinness of the film thickness), $T_S(z)$ is the temperature of the substrate at a distance z from the interface, c_f and c_s are specific heats of the film and substrate, and λ_s is the thermal conductivity of the substrate. Equation (2) relates the heat flux across the interface to the Kapitza conductance Λ_{Bd} , whereas equation (3) describes thermal diffusion in the substrate. Heat flow parallel to the interface and heat loss from the surface of the metal are neglected. These simplifications are allowed due to the small time scales. The substrate is treated as semi-infinite, because less than $2 \mu\text{m}$ of the substrate are influenced by the temperature rise on the 1–2 ns timescale of the experiment.

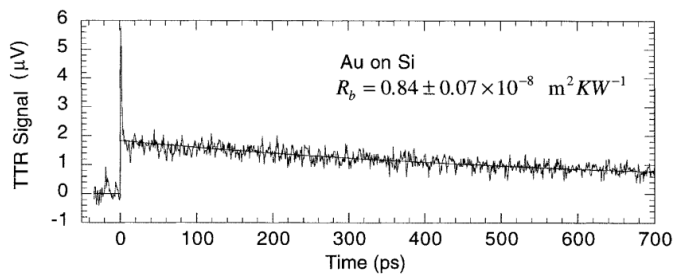


Figure 4: TTR signal curves and fitted thermal model curves for Au/SiO₂ and Au/Si samples (Reprinted by permission of the publisher from [15]. Published by Taylor & Francis Ltd, <http://tandf.co.uk/journals>)

Equations (2) and (3) can be solved numerically to obtain the cooling curve of the metal. The computer algorithm fits the analytical curve to the experimental one, as the Kapitza conductance (the inverse of ITR) is treated as a free parameter. This procedure

yields the value of the film-substrate interfacial thermal resistance, denoted as R_b in Fig. 4. This technique relies on the shape of the cooling profile, since the signal is proportional to the change in temperature and the proportionality constant is not known precisely. The thermal model must be scaled to the experimental data at some point. Ideally the scaling point will not affect the results, although a variance of 5% in the measured values was found when the scaling point was changed throughout the data used in the curvefit. The first 15 ps are not used in the least-squares fitting routine, because the presence of strain can influence the reflectivity response within this period [15].

In order to resolve the interfacial thermal resistance, the time constant of the film should be significantly smaller than the time constant associated with the interface. This condition puts a limitation on the maximum film thickness. According to Stevens et al. [17] the validity of the experimental technique is limited to the situations where:

$$\frac{\tau}{\tau_{Bd}} < 1 \quad (4)$$

The time constants, τ of the film and τ_{Bd} of the interface, may be expressed as:

$$\tau = \frac{d^2}{\alpha} \quad (5)$$

and

$$\tau_{Bd} = \frac{C_f d}{\lambda_{Bd}} \quad (6)$$

where d is the film thickness, α is the effective diffusivity of the film, C_f is the thermal capacitance of the film and λ_{Bd} is the inverse of interfacial thermal resistance. Practically, for interfaces with $\lambda_{Bd} \approx 2 \times 10^8 \text{ W}/(\text{m}^2\text{K})$ this limits maximal d to 100 nm. Film thickness is also limited by the fact that the time constant should be smaller than or of the order of the TTR scan length, which for scan lengths of 1–2 ns limits the maximum value of d again to 100 nm [17].

If the thermal conductivity of the substrate is too low (lower than $25 \text{ W}/(\text{m}\cdot\text{K})$), the internal thermal resistance of the substrate may dominate over the interfacial thermal resistance in the influence on the

observed temperature decay. High thermal conductivity also reduces issues associated with steady-state heating. This condition eliminates the use of glasses for substrate materials [17]. Nevertheless, the presented method has proven to be an effective and reliable way of determining ITR between metals and dielectrics. Its advantage is the fact that it has been used for more than twenty years and its subtleties are quite well understood.

4.3. Modulated thermorefectance

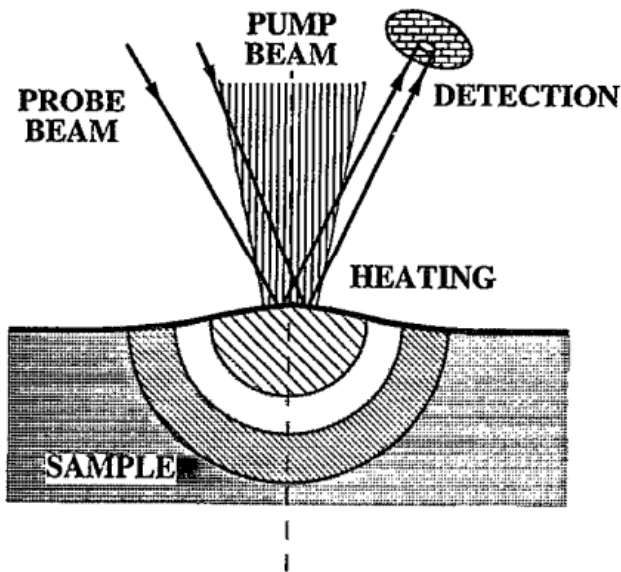


Figure 5: The principle of modulated thermorefectance measurement (Reprinted with permission from [18]. Copyright © 1995, American Institute of Physics). Note the presence of photoelastic deformation due to heating

The modulated thermorefectance method, also known as modulated optical reflectance (MR) or modulated photorefectance, is a method of thermal characterization of materials which utilizes the same physical phenomenon as the previous method (TTR). The experimental setup for the method is very similar to the TTR setup. A mono- or multilayer sample is heated by one laser beam (the pump beam). This time the heating is continuous and not by impulse. The intensity of the heating beam is periodically modulated at some fixed frequency. This type of heating triggers the formation of thermal waves in the sample. The thermal waves in the sample are sensed using a weaker laser beam (probe beam), which reflects off the surface of the sample and is

gathered by a detector. The intensity of reflected light depends on the optical reflectivity of the sample which changes with temperature. The recorded signal is therefore temperature-dependent. In Fig. 5, the diagram of the measurement is presented. It is shown that the probe beam is directed at the point of excitation, but it may also be directed at some other point near the excitation point.

Thermal properties of the sample material are computed based on the signal phase data while precise data about the amplitude of the signal is not crucial in general. Modulated continuous heating results in a simpler mathematical model than pulse heating, but the accumulation of heat in the sample may cause a temperature increase and an unwanted change in its thermophysical properties. For that reason it is important to use sufficiently short heating times and low beam energies. The technique is most widely used for thermal diffusivity measurement in solid materials. The thermal diffusivity α of an optically and thermally thick, isotropic, bulk material can be readily deduced from the slope of the signal phase φ versus the distance x from the excitation point ($d\varphi/dx = \sqrt{\pi f/\alpha}$, where f is the pump modulation frequency) [19]. Characterization of film/substrate samples is also possible. In the case of a thin film on substrate, the measured apparent diffusivity is in fact a nontrivial function of the diffusivities of the film and the substrate, and the ITR between them. Early models made it possible to calculate the thermal diffusivity of one of the layers when the thermal diffusivity of the other layer and the ITR are known. In practice, was hard to achieve good accuracy with this calculation as the input parameters (the ITR and diffusivity of one layer) had to be obtained from another measurement or the literature and did not always agree with the actual sample data. To remove that uncertainty a model was developed which allows for the simultaneous calculation of all three unknown thermal properties for a given sample. The details of the thermal model can be found in [20]. To obtain the desired thermal properties of the film/substrate sample, the phase profile must be measured at several different modulation frequencies (at least three) covering an appropriate range. In addition, when the film is thermally anisotropic, a rough estimate of the anisotropy magnitude may also be obtained by com-

paring the measured with the predicted amplitudes.

Li et al. [19] used this method to measure the thermal diffusivities and the ITR for thin films of gold (78 nm) or YBaCuO (300 nm) on LaAlO₃ substrate. The procedure they followed will be briefly described. At fixed modulation frequency, the amplitude and phase data are recorded for 30–40 different separations between pump and probe beams. The process is repeated for 4–6 modulation frequencies from the 1 kHz–1 MHz range. A curve from a rigorous thermal model is then fitted to the collected data points by a least squares method. The sought thermal properties are treated as free parameters. Since it is well known that the phases are less dependent on nonthermal features than the amplitudes, only the phase data was actually fitted. The amplitudes were then used to test the quality of the obtained fit.

Reproducibility and sensitivity tests performed by Li et al. show that for the thermal characterization of film/substrate samples whose film and substrate diffusivities are comparable, a simultaneous accurate determination of the substrate diffusivity is essential for a correct determination of the film diffusivity and of the ITR. If the substrate diffusivity is estimated accurately, the errors regarding the remaining unknowns are small. In conclusion, the method gives relatively good estimates when used carefully and has some undeniable strengths, namely its non-destructive, noncontact nature and high spatial resolution. The modulated thermorefectance was also used by Meyer-Berg et al. [21] to estimate the thermal boundary resistance between grain boundaries in thin films of aluminum (1% Si, 0.5% Cu), deposited on the SiO₂ substrate.

4.4. Semi-intrinsic thermocouple measurement

This technique presented by Garnier et al. [22] is one of the few in which samples taken from actual composite material are used. The authors remarked that contact measurement of temperature of the interesting point on the sample, by a thermal probe, such as used in scanning thermal microscopy, is not useful in the case of ITR measurement. This is due to parasitic probe-sample thermal resistance which is of the order of the measured interfacial thermal resistance. Thus, the associated error is too large to estimate ITR accurately. They proposed a method

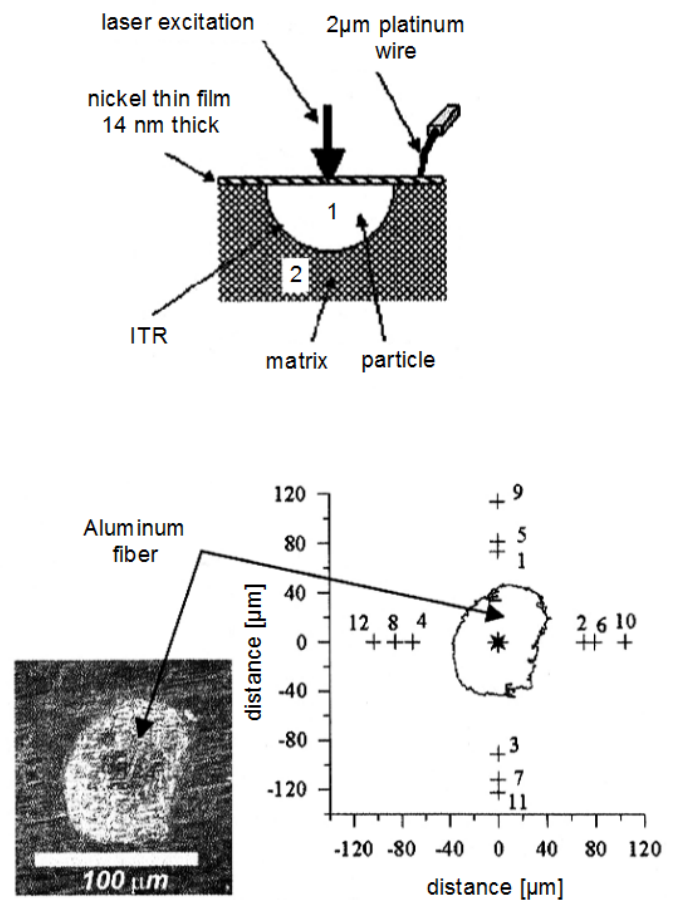


Figure 6: Experimental setup and locations of the temperature phase lag measurements. Adopted from [22]

to reduce the probe-sample resistance by coating the composite with a thin (14 nm) nickel film. The film forms part of the thermocouple. The other part is a thin platinum wire (2 μm) which, in contact with the coating, provides thermoelectric effects when the heat flow is induced in the sample by laser excitation. The setup is presented in Fig. 6.

The laser beam of intensity modulated at frequency f is directed at a particle or fiber. In the original experiment the filler considered was a metal and the matrix a polymer. Harmonic heat flow is generated in the sample and the temperature phase lag is recorded for several different locations in the matrix region of the surface. The locations where temperature phase lags were measured by the thin platinum wire probe are shown in Fig. 6.

The thermal resistance between nickel coating and polymer is estimated to be of the order of 10–

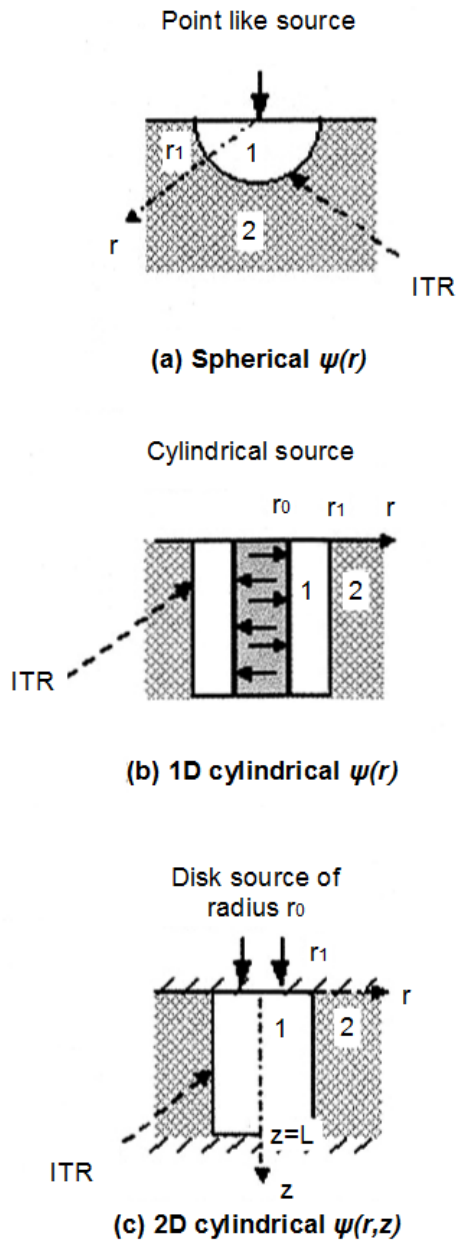


Figure 7: Geometry and boundary conditions of considered thermal models. 1—reinforcement, 2—matrix, ψ —temperature phase lag. Adopted from [22]

$7 \text{ m}^2\cdot\text{K}/\text{W}$, which seems to be negligible compared to the filler matrix ITR finally obtained [22]. Thermal contact between filler and matrix is usually imperfect in composites of this type. The interface strongly affects the heat flow. By comparing the recorded temperature phase lag data with theoretical models one is able to estimate the filler-matrix ITR. Garnier and co-authors proposed three mathematical models from which the ITR value may be extracted. Cylin-

dricl 1D or 2D and spherical 1D heat transfer models were simulated, with different types of boundary conditions and geometry, as shown in Fig. 7.

The matrix was considered a semi-infinite solid, except in the z -direction (i.e. for $z = L$) of the 2D cylindrical model where convergence is easier for the finite medium. Radiative and convective heat transfer is neglected because of the small temperature rise and the fact that the period of the harmonic part of the heat flow is much smaller than the time constant required for convection settling [22]. The details of thermal models may be found in [22].

Table 1: Values of ITR calculated using different thermal models [22]

f , Hz	Particle/matrix interfacial thermal resistance, $10^{-5} \text{ m}^2\cdot\text{K}/\text{W}$	Spherical model	Cylindrical 1D	Cylindrical 2D
0.1		49	1.6	3.6
0.2		24	1.9	3.0
0.5		15	2.8	3.3
1		18	4.9	5.2
2		14	5.3	5.4

As expected, the spherical model result differs greatly from the result obtained with the use of cylindrical models. One may see that values of ITR from cylindrical models are quite close while the values from the spherical model are much higher (See Table 1 for calculated ITR).

The measured ITR does not change with the thermocouple location. Table 1 shows the obtained ITR values for different modulation frequencies f . At lower frequencies, results obtained by both spherical and 1D cylindrical models are biased because the thermal length δ_1 in aluminum is greater than the fiber radius or fiber length.

By performing the uncertainty analysis and averaging, the authors were able to obtain an average value of ITR for the given composite sample. It was estimated to be $(3.81 \pm 0.59) \times 10^{-5} \text{ m}^2\text{K}/\text{W}$. The result is close to the one reported by Chapelle et al. [6] for a polymer-metal composite (0.3×10^{-5} and $1.6 \cdot 10^{-5} \text{ m}^2\cdot\text{K}/\text{W}$). It appears that ITR values for typical particulate composites are generally higher than

the values for thin films deposited onto substrates where R_{Bd} is of the order of $10^{-7} \text{ m}^2 \cdot \text{K}/\text{W}$ [13]. The difference is most likely caused by the imperfections (e.g., unsticking areas) at the interfaces between filler and matrix, while for the film-substrate interfaces the quality of the bond is higher and hence the phonon scattering is lower.

4.5. Hot wire method

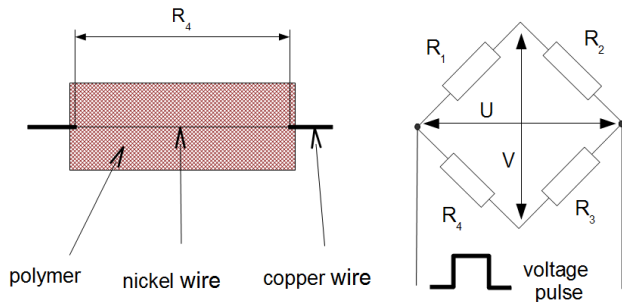


Figure 8: The principle of ITR measurement between metallic wire and polymer matrix by the hot wire method; adopted from [6]

Chapelle et al. [6] proposed the use of the hot wire method for ITR estimation in polymer matrix composites reinforced by metallic fiber. The technique requires preparation of cylindrical samples where metallic wire is embedded in polymer matrix. It is intended to simulate the matrix-fiber joint of a typical composite. The metallic wire is installed as a branch of a Wheatstone bridge. A voltage pulse provides heating by the Joule effect. The average temperature of the wire T , and the electric power P_0 , are calculated based on two voltage measurements: the supplying voltage U and unbalanced voltage V (See Fig. 8). The relationship between T and V/U is obtained by recording the changes of V while low supply voltage U is provided and the temperature of the sample is varied (for this purpose, the sample is placed in a temperature controlled enclosure). The ITR is obtained from the thermal model, where the inputs are temperature T and electrical power P_0 measurements.

In the thermal model it is assumed that the heat transfer is one-dimensional, as the wire's length-to-diameter ratio is high (of the order of 1000). The wires tested were of nickel with diameters of 26.9, 55.8 and 122.9 μm and lengths L respectively of 25,

50 and 161 mm. The matrix (epoxy resin) surrounding the wire is treated as semi-infinite. This is justified because of the short heating time of 10 ms, which corresponds to thermal diffusion length of about 40 μm —far lower than the radius of the cylinder (8 mm).

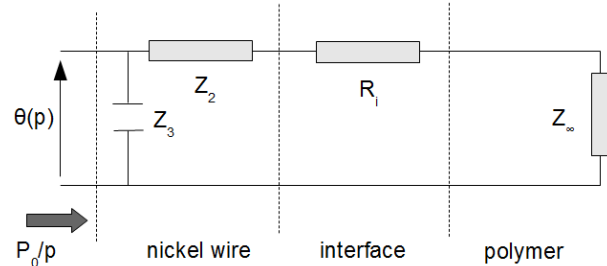


Figure 9: The impedance network representing the heat transfer in the sample; adopted from [6]

The model has to provide the average of the temperature of the wire taken along the full length of the wire. The matrix-fiber system can be represented by the impedance network shown in Fig. 9.

The average temperature of the wire is at first calculated in the Laplace domain, by the thermal quadrupoles technique [23]. It may be written as:

$$\theta(p, R_{Bd}) = \frac{P_0}{p} \frac{1}{(1/Z_3) + (1/(Z_2 + (R_{Bd}/\pi\phi_{Ni}L) + Z_\infty))} \quad (7)$$

where:

$$Z_3 = \frac{4}{\rho_{Ni}C_{pNi}\pi\phi_{Ni}^2Lp} \quad (8)$$

$$Z_2 = \frac{I_0(s)}{2\pi\lambda_{Ni}LsI_1(s)} - Z_3 \quad (9)$$

$$Z_\infty = \frac{K_0(s')}{2\pi\lambda_{ep}Ls'K_1(s')} \quad (10)$$

$s = (\phi_{Ni}/2) \sqrt{(p/\alpha_{Ni})}$, $s' = (\phi_{Ni}/2) \sqrt{(p/\alpha_{ep})}$, p is the Laplace variable, I_0 , K_0 and K_1 are Bessel functions, P_0 is the electrical power dissipated in the wire, ϕ_{Ni} is its diameter, λ_{Ni} and λ_{ep} are thermal conductivities of nickel (wire) and the epoxy resin, α_{Ni} and α_{ep} are thermal diffusivities, and ρC_{pNi} and ρC_{pep} are the volumetric specific heats of nickel (Ni) and epoxy resin (ep).

The next step is taking the temperature θ to the time domain, where it is denoted by T . This can be achieved numerically with the help of the Gaver-Stehfest algorithm:

$$T(t, R_{Bd}) = \frac{\ln(2)}{t} \sum_{j=1}^n V_j \theta\left(\frac{j \ln(2)}{t}, R_{Bd}\right) \quad (11)$$

where:

$$V_j = (-1)^{(n/2+1)} \sum_{k=\lfloor \frac{j+1}{2} \rfloor}^{\min(j, \frac{n}{2})} \frac{k^{\binom{n}{2}+1} (2k)!}{(n/2 - k)! k! (j - k)! (2k - 1)!} \quad (12)$$

Given the measured T and P_0 values, the interfacial thermal resistance R_{Bd} can be calculated from the above thermal model. It is good when the rise in the temperature of the wire is small (the final rise was about 2 K), then we can assume that the thermophysical properties of the material remain constant.

The analysis of sensitivity and reproducibility performed by Chapelle et al. showed that the most influential possible source of error is axial heat loss, which should theoretically be negligible due to the high length-to-diameter ratio of the wire. The biases on the computed ITR value, connected with the axial heat loss effect, are estimated to be of order of 7%. The biases may be corrected by using two wires of different length or by performing a 2D finite element simulation of the experiment. For details, see the original paper [6].

In the measurements of ITR with application to composites, it is critical to accurately recreate the interfacial pressures and condition of the interface (roughness) existing in the actual composite. The presented technique uses samples that seem to satisfy these crucial requirements well, which is a big advantage, especially knowing that the measurement of interfacial contact pressures in composites is not practically possible [6]. Another strong side of this method is the good analysis of uncertainties, sensitivity and error sources made by the authors, which raises the degree of reliability.

4.6. Macromodel method

Due to the size of filler particles in modern composites for heat conduction, it is quite difficult to

perform any direct measurement regarding the filler-matrix interface. In most cases, microscopic methods are required. To resolve this inconvenience in the case of estimating experimental filler-matrix ITR, Hill and Supancic [24] proposed that it is valid to measure the ITR in the enlarged model of the filler-matrix joint (the “macromodel”) and relate the result to the ITR in the composite material. Their assumption is that prepared models allow for good simulation of the interfacial conditions present in the composite, and the ITR measured using the macromodels should be more or less equal to the filler-matrix ITR in the composite.

Their experiment involved composites with polymer matrix and ceramic filler particles. To perform the measurements, sandwich structures were prepared where epoxy resin was sandwiched between two sapphire wafers. To achieve a thin, even layer of epoxy on a circular wafer, the spin-coating technique was utilized. The two epoxy-coated wafers were then placed together face to face to form the sandwich structure (the epoxy coated surfaces joined). The structure was then annealed at 100°C, which is below the polymerization temperature, which allowed the epoxy layer to melt and flow to form a uniform layer. Any excess epoxy was removed by solvent. The last step in the preparation was thermal treatment at 170°C to obtain polymerization of the epoxy.

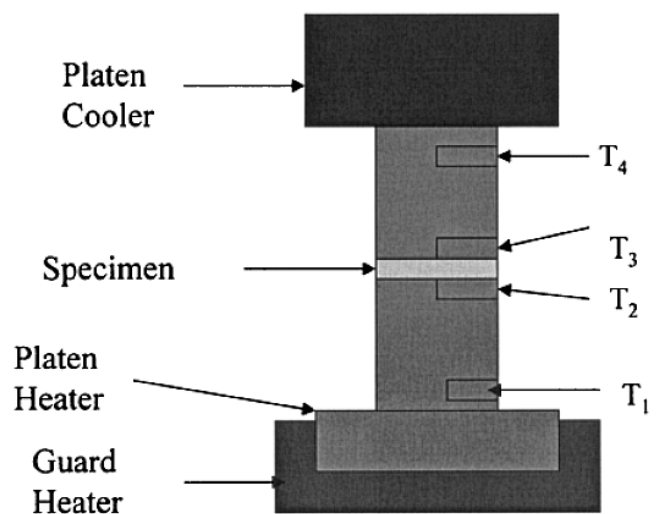


Figure 10: Diagram of steady state thermal resistance measurement apparatus (Reprinted with permission from [24]. Copyright © 2005, John Wiley and Sons)

The thermal resistance in the macromodels was measured with a typical steady state apparatus. The principle of measurement is shown in Fig. 10. The sample is placed between two highly polished nickel-coated copper platens in which four thermocouples (T_1 – T_4) are installed to record the gradient of temperature. It is pressed with a force of 0.22 kN, corresponding to a pressure of 0.35 MPa. To decrease the thermal contact resistance between the platens and outer surfaces of the sample, a 0.05 mm thick metallic alloy foil that melts at 60°C was placed between the platens and both surfaces of the macromodels. It serves as thermal interface material (TIM) and proved to work better than commercial TIM.

The total resistance R_T measured by the apparatus may be written as a sum of resistances:

$$R_T = 2R_{PS} + 2R_S + R_E + 2R_{ES} \quad (13)$$

where R_{PS} is the thermal resistance between the nickel-coated platen and sapphire wafer, R_S is the thermal resistance of a sapphire wafer, R_E is the thermal resistance of the epoxy layer and R_{ES} is the ITR between epoxy resin and sapphire wafer. From this expression the ITR between epoxy and ceramic wafer (R_{ES}) can be easily obtained, knowing the remaining resistances.

The thermal resistance of material layers may be calculated knowing the thicknesses and thermal conductivities of the layers. These can be measured in separate experiments. So we have $R_E = dE/\lambda E$ and $R_S = dS/\lambda S$, where dE and dS are thicknesses, and λE and λS are thermal conductivities of epoxy and sapphire, respectively.

Estimation of the platen-sapphire thermal resistance R_{PS} is slightly more complicated and requires some attention. First of all the R_{PS} has to be heavily reduced. This Hill and Supancic achieved by using the thin metallic foil as a TIM. The use of typical thermal grease did not guarantee the thermal resistance reduction or the reproducibility of results required to estimate R_{ES} with appropriate certainty. To attain R_{PS} , a single sapphire wafer was placed between the test apparatus platens, with the metallic foils between both contact surfaces. When the test apparatus was heated to the steady-state operating temperature of $\sim 90^\circ\text{C}$, the foil melted, and most

of the alloy was squeezed out, leaving behind only a very thin film of alloy that filled in the surface irregularities of the platens and sapphire wafer. The total thermal resistance measured with this type of setup is expressed by

$$R_T = R_S + 2R_{PS} \quad (14)$$

Once again, the R_S may be calculated based on the wafer's thickness and thermal conductivity measurement. Then we can easily obtain R_{PS} from the above equation. Repeating the measurement for few wafers gives additional accuracy. It is assumed that the same value of R_{PS} applies to the measurements on the wafer-epoxy-wafer samples as the contacting surfaces, and their treatment are identical.

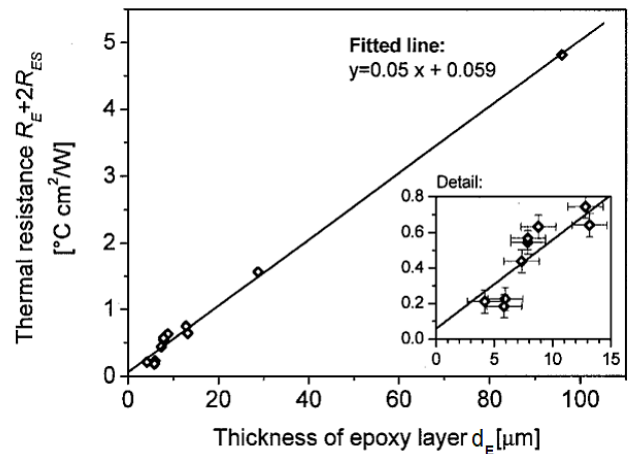


Figure 11: Thermal resistance as a function of epoxy layer thickness (Reprinted with permission from [24]. Copyright © 2005, John Wiley and Sons)

The values of R_T , R_S and $2R_{PS}$ can now be substituted to (13), allowing one to calculate the sum $R_E + 2R_{ES}$ for each macromodel. Hill and Supancic plotted the data on $R_E + 2R_{ES}$ as a function of the thickness of the epoxy layer for each macromodel, including the error bars in both directions (Fig. 11). Then a nonlinear fitting routine was used to obtain a correct straight line with respect to the statistical weights. The point where the best fit line intersects the vertical axis (the thermal resistance for zero thickness of epoxy layer) is the approximate value of $2R_{ES}$, while the reciprocal value of the slope of the line corresponds to the thermal conductivity of the epoxy material.

From the plot it was estimated that the $2R_{ES}$ between sapphire and epoxy is $0.06^\circ\text{C cm}^2/\text{W}$ at $90^\circ\text{--}100^\circ\text{C}$. R_{ES} is half of this value or $0.03^\circ\text{C cm}^2/\text{W}$, showing a standard deviation of about 0.018. The error analysis shows that, among possible error sources, the platen-to-sapphire thermal resistance R_{PS} has the highest influence on the final R_{ES} value and thus requires careful estimation.

The strengths of the macromodel method of matrix-filler ITR determination in composites are: the simple principle of measurement, the absence of a complex mathematical model and no requirement of miniaturization. One possible weakness is the assumption of equality of the ITR in the macromodels and ITR in the composite material. No evidence was presented by the authors to support the validity of this assumption, and yet there are reports which show that filler-matrix ITR does depend on the geometry (the size of particles; see [6]). We may treat the planar interface present in the macromodels as an interface of a particle with infinite radius, whereas the radius of ordinary filler particles is finite.

4.7. The flash method

The flash method is a fast and popular method of thermal diffusivity measurement for various technical materials. Given the thermal diffusivity α , the thermal conductivity of the sample λ can be easily computed from $\alpha = \lambda/\rho c_p$, where ρ is the density and c_p is specific heat at constant pressure. To measure diffusivity at high temperatures, the test apparatus may be equipped with a furnace. The technique uses thin cylindrical samples (diameter ~ 12.5 mm, 3 to 10 mm high). One side of the sample is heated by a short laser or Xenon lamp pulse and the temperature response on the reverse side of the sample is recorded by an infrared sensor. The thermal diffusivity of the sample is then computed from the shape of the recorded temperature curve. Numerous thermal models have been developed for this purpose, including the original model by Parker et al. [25] and its refined versions by Cowan [26] and Cape and Lehman [27].

The diagram showing the principle of measurement is presented in Fig. 12. In the basic model, by Parker et al. [25], the thermal diffusivity of the sample is calculated based on only one parameter of the

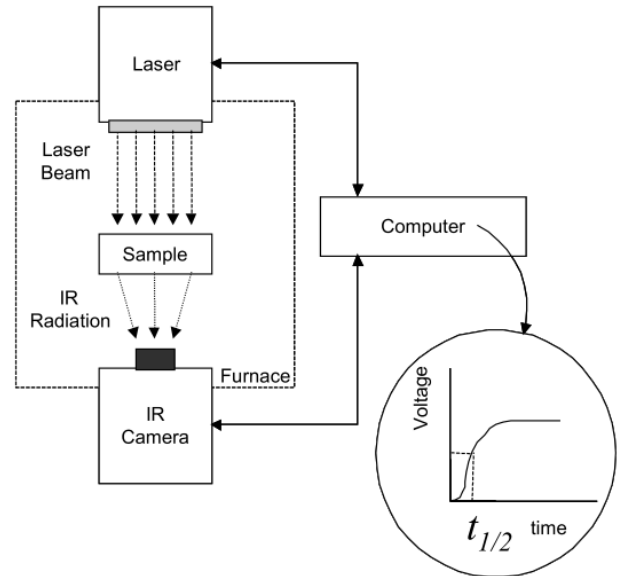


Figure 12: Experimental setup for laser flash method of thermal diffusivity measurement (Reprinted from [28]. Copyright © 2002, with permission from Elsevier)

curve—the time $t_{1/2}$ in which the reverse-side temperature reaches one-half of its maximum value. The equation is $\alpha = 1.388 L^2 / (\pi^2 t_{1/2})$, where L is the sample thickness. The simplicity of the model reduces the chance of error. In the Parker model it is assumed that the sample is thermally isolated from the environment, its thermo-physical properties remain constant during the experiment, the pulse time is infinitely small and the entirety of the radiation is absorbed in the thin layer of material near the surface. Cowan [26] added the correction regarding heat losses from both the upper and lower surfaces of the sample, while Cape and Lehman [27] analyzed the effects of radiation at high temperatures, finite duration of the heating pulse, and the feasibility of low temperature measurements.

Due to the popularity of the technique and the availability of commercial laser flash measurement systems, some researchers explored the possibility of applying it to multilayer or inhomogeneous samples. Among these there are three main approaches. The first approach is to measure the thermal diffusivity of the layered sample, by the laser flash method, treating it as homogeneous—e.g., using the thermal model for single-layer samples. This approach was utilized by Chiu et al. [28]. In their experiment, they estimated the ITR between Cu and Solder in

Cu/Solder/Cu sandwich samples. They measured the effective thermal conductivity of the sample and, knowing the bulk thermal resistances of Cu and solder, were able to calculate the total thermal resistance R_t of the solder layer. The total resistance of the solder layer can be expressed as the bulk resistance of the solder plus the interfacial resistances of two interfaces. By making series of measurements one is able to obtain the graph of R_t versus the solder thickness and draw a straight line of regression. The point where the line intersects the vertical axis (the R_t for zero solder thickness) is an approximation of two times the ITR between Cu and solder. We must note however, that it is not always valid to treat multilayer samples as homogeneous. A more detailed discussion on this topic can be found in [29].

A second approach to measuring ITR through laser flash analysis is by using thermal models designed specifically for two- or three-layer samples. These allow one to measure the thermal diffusivity of one of the layers if the thermal diffusivities of the other layers are known. The computation of interfacial thermal resistance in a layered sample is possible. Basic models for this case have been proposed by Lee [30] and Hartmann et al. [31]. The approach has been explored further by Milosević et al. [32–34]. In the most popular approach [31], the theoretical temperature curve is nonlinearly fitted to the complete measured temperature history, instead of just using $t_{1/2}$. To perform the fit one must know the densities, specific heats, thermal diffusivities and thicknesses for every layer. This type of measurement has been employed by Tao et al. [35] to measure ITR of copper/graphite samples.

Another possibility is to measure the effective thermal conductivity, based on the thermal diffusivity measurement, of specimens taken from an interesting particulate composite material. It is important to ensure that the sample may be treated as nearly homogeneous, e.g., the diameter of the particles should be much lower than the thickness of the sample. Given the effective thermal conductivity of the composite, measured with the aid of the flash method, and the thermo-physical properties of constituent materials, the average ITR can be calculated using one of available thermal conductivity models for composites (See [8]).

5. Summary

Multiple techniques for determining interfacial thermal resistance, with possible application to composite materials, have been presented. The interfacial thermal resistance between filler and matrix is a combination of thermal boundary resistance dependent on the physical properties of constituent phases and thermal contact resistance caused by imperfect mechanical and chemical bonding. In an ideal case, the value of ITR between two given joined materials should always be identical. In practice, poor reproducibility is often encountered. This is mainly due to the high dependence of ITR on interfacial parameters such as roughness and contact pressures, which are hard to recreate, and even scale effects, with the role of each still being unclear.

The approaches to experimental evaluation of ITR in composite materials may then be separated into two categories. In the first category we have approaches in which samples made of target composite material are used. A method of this type is described in [22] but indirect ITR estimations based on thermal conductivity measurements may also be included here [7–12]. A second approach is to measure the ITR in samples made of the same materials as the target composite, to mimic the filler-matrix joint, but often with different geometry and scale than that of the target composite. Here we may include film-on-substrate measurements [13, 15–17, 19], the hot wire method [6], the macromodel method [24] and the laser flash method [28–35]. As for these methods, the measured average ITR may differ from that present in the target composite material.

It is observed that ITR in composites changes locally along the interface. This is true especially for metal matrix composites filled with diamond particles, where different walls of the same particle have different adhesion [36, 37]. An ideal measurement technique should allow for local ITR measurement in samples taken directly from the target composite. It was pointed out that local measurement of ITR by scanning thermal microscopy is currently impossible due to parasite probe-sample contact resistance. For the same reason it is better to use non-contact methods, e.g., the optical or infrared method, to measure of temperature in ITR measurements.

Acknowledgments

This work has been supported by the National Centre for Research and Development within the European Regional Development Fund under the Operational Program Innovative Economy No. POIG.01.01.02-00-097/09 “TERMET—New structural materials with enhanced thermal conductivity”.

References

- [1] G. Bai, W. Jiang, L. Chen, Effect of interfacial thermal resistance on effective thermal conductivity of MoSi₂/SiC composites, *Materials Transactions* 47 (4) (2006) 1247–1249.
- [2] E. T. Swarz, R. O. Pohl, Thermal boundary resistance, *Reviews of Modern Physics* 61 (3) (1989) 605–668.
- [3] R. S. Prasher, P. E. Phelan, A scattering-mediated acoustic mismatch model for the prediction of thermal boundary resistance, *Journal of Heat Transfer* 123 (1) (2001) 105–112.
- [4] P. Furmański, T. S. Wiśniewski, J. Banaszek, Thermal contact resistance and other thermal phenomena at solid-solid interface, *Institute of Heat Engineering, Warsaw, 2008*.
- [5] D. G. Cahill, W. K. Ford, K. E. Goodson, G. D. Mahan, A. Majumdar, H. J. Maris, R. Merlin, S. R. Phillpot, Nanoscale thermal transport, *Journal of Applied Physics* 93 (2003) 793.
- [6] E. Chappelle, B. Garnier, B. Bourouga, Interfacial thermal resistance measurement between metallic wire and polymer in polymer matrix composites, *International Journal of Thermal Sciences* 48 (12) (2009) 2221–2227.
- [7] H. Bhatt, K. Y. Donaldson, D. P. H. Hasselman, Role of interfacial carbon layer in the thermal diffusivity/conductivity of silicon carbide fiber-reinforced reaction-bonded silicon nitride matrix composites, *Journal of the American Ceramic Society* 75 (2) (1992) 334–340.
- [8] C.-W. Nan, X.-P. Li, R. Birringer, Inverse problem for composites with imperfect interface: determination of interfacial thermal resistance, thermal conductivity of constituents, and microstructural parameters, *Journal of the American Ceramic Society* 83 (4) (2000) 848–854.
- [9] K. Jagannadham, H. Wang, Thermal resistance of interfaces in AlN–diamond thin film composites, *Journal of Applied Physics* 91 (2002) 1224–1235.
- [10] F. Macedo, J. A. Ferreira, Thermal contact resistance evaluation in polymer-based carbon fiber composites, *Review of Scientific Instruments* 74 (1) (2003) 828–830.
- [11] M. Kida, L. Weber, C. Monachon, A. Mortensen, Thermal conductivity and interfacial conductance of AlN particle reinforced metal matrix composites, *Journal of Applied Physics* 109 (2011) 064907.
- [12] A. M. Abyzov, S. V. Kidalov, F. M. Shakhov, Filler-matrix thermal boundary resistance of diamond-copper composite with high thermal conductivity, *Physics of the Solid State* 54 (1) (2012) 210–215.
- [13] E. T. Swarz, R. O. Pohl, Thermal resistance at interfaces, *Applied Physics Letters* 51 (1987) 2200.
- [14] K. E. Goodson, M. I. Flik, L. T. Su, D. A. Antoniadis, Annealing-temperature dependence of the thermal conductivity of LPCVD silicon-dioxide layers, *Electron Device Letters, IEEE* 14 (10) (1993) 490–492.
- [15] A. N. Smith, J. L. Hostetler, P. M. Norris, Thermal boundary resistance measurements using a transient thermoreflectance technique, *Microscale Thermophysical Engineering* 4 (1) (2000) 51–60.
- [16] R. J. Stoner, H. J. Maris, Kapitza conductance and heat flow between solids at temperatures from 50 to 300 K, *Physical Review B* 48 (22) (1993) 16373.
- [17] R. J. Stevens, A. N. Smith, P. M. Norris, Measurement of thermal boundary conductance of a series of metal-dielectric interfaces by the transient thermoreflectance technique, *Journal of Heat Transfer* 127 (3) (2005) 315–322.
- [18] F. Lepoutre, D. Balageas, P. Forge, S. Hirschi, J. L. Joulaud, D. Rochais, F. C. Chen, Micronscale thermal characterizations of interfaces parallel or perpendicular to the surface, *Journal of Applied Physics* 78 (1995) 2208.
- [19] B. Li, J. P. Roger, L. Pottier, D. Fournier, Complete thermal characterization of film-on-substrate system by modulated thermoreflectance microscopy and multiparameter fitting, *Journal of Applied Physics* 86 (1999) 5314.
- [20] B. Li, S. Zhang, The effect of interface resistances on thermal wave propagation in multi-layered samples, *Journal of Physics D: Applied Physics* 30 (1997) 1447–1454.
- [21] G. Meyer-Berg, R. Osiander, P. Korpiun, P. Kakoschke, H. Joswig, *Springer series in Optical Sciences, Vol. 69, Springer, Berlin, 1992, Ch. The thermal resistance of grain boundaries determined by modulated optical reflectance, pp. 711–713*.
- [22] B. Garnier, T. Dupuis, J. Gilles, J. P. Bardou, F. Danes, Thermal contact resistance between matrix and particle in composite materials measured by a thermal microscopic method using semi-intrinsic thermocouple, in: *Proceedings of the 12th International Heat Transfer Conference, Grenoble, France, 2002, pp. 9–14*.
- [23] D. Maillet, S. Andre, J.-C. Batsale, A. Degiovanni, C. Moyne, *Thermal quadrupoles, Wiley, Chichester, 2000*.
- [24] R. F. Hill, P. H. Supancic, Determination of the thermal resistance of the polymer–ceramic interface of alumina-filled polymer composites, *Journal of the American Ceramic Society* 87 (10) (2004) 1831–1835.
- [25] W. J. Parker, R. J. Jenkins, C. P. Butler, G. L. Abbott, Flash method of determining thermal diffusivity, heat capacity, and thermal conductivity, *Journal of Applied Physics* 32 (9) (1961) 1679–1684.
- [26] R. D. Cowan, Pulse method of measuring thermal diffusivity at high temperatures, *Journal of Applied Physics*

- 34 (4) (1963) 926–927.
- [27] J. A. Cape, G. Lehman, Temperature and finite-time effects in the flash method for measuring thermal diffusivity, *Journal of Applied Physics* 34 (1963) 1909–1913.
- [28] C.-P. Chiu, J. G. Maveety, Q. A. Tran, Characterization of solder interfaces using laser flash metrology, *Microelectronics Reliability* 42 (2002) 93–100.
- [29] J. Absi, D. S. Smith, B. Nait-Ali, S. Grandjean, J. Berjon-naux, Thermal response of two-layer systems: Numerical simulation and experimental validation, *Journal of the European Ceramic Society* 25 (2005) 367–373.
- [30] H. J. Lee, Thermal diffusivity in layered and dispersed composites, Ph.D. thesis, Purdue University, Lafayette, Indiana (1975).
- [31] J. Hartmann, O. Nilsson, J. Fricke, Thermal diffusivity measurements on two-layered and three-layered systems with the laser flash method, *High Temperatures-High Pressures* 25 (1993) 403–410.
- [32] N. D. Milosević, M. Raynaud, K. D. Maglić, Simultaneous estimation of the thermal diffusivity and thermal contact resistance of thin solid films and coatings using the two-dimensional flash method, *International Journal of Thermophysics* 24 (3) (2003) 799–819.
- [33] N. D. Milosević, Optimal parametrization in the measurements of the thermal diffusivity of thermal barrier coatings, *Thermal Science* 11 (1) (2007) 137–156.
- [34] N. D. Milosević, Determination of transient thermal interface resistance between two bonded metal bodies using the laser-flash method, *International Journal of Thermophysics* 29 (2008) 2072–2087.
- [35] Z. Tao, Q. Guo, X. Gao, L. Liu, The wettability and interface thermal resistance of copper/graphite system with an addition of chromium, *Materials Chemistry and Physics* 128 (2011) 228–232.
- [36] P. W. Ruch, O. Beffort, S. Kleiner, L. Weber, P. J. Uggowitzer, Selective interfacial bonding in Al(Si)–diamond composites and its effect on thermal conductivity, *Composites Science and Technology* 66 (2006) 2677–2685.
- [37] K. Chu, C. Jia, X. Liang, H. Chen, W. Gao, H. Guo, Modeling the thermal conductivity of diamond reinforced aluminium matrix composites with inhomogeneous interfacial conductance, *Materials and Design* 30 (2009) 4311–4316.
- ρ density
- τ time constant
- θ temperature (Laplace domain)
- φ, ψ signal phase
- A area
- C thermal capacitance
- c specific heat
- d thickness
- f frequency
- I, i electric current
- L length
- P power
- p Laplace variable
- R thermal resistance
- r optical reflectivity
- T temperature
- t time
- U, V voltage
- Z impedance
- z distance (spatial coordinate)

Nomenclature

- α thermal diffusivity
- \dot{Q} heat rate
- Λ thermal conductance
- λ thermal conductivity
- ϕ diameter